



# Health assessment and ambient vibration testing of the “Ponte delle Torri” of Spoleto during the 2016–2017 Central Italy seismic sequence

Ivan Roselli<sup>1</sup> · Marialaura Malena<sup>2</sup> · Marialuisa Mongelli<sup>1</sup> · Nicola Cavalagli<sup>3</sup> · Massimiliano Gioffrè<sup>3</sup> · Gerardo De Canio<sup>1</sup> · Gianmarco de Felice<sup>2</sup>

Received: 10 July 2017 / Accepted: 3 January 2018 / Published online: 24 January 2018  
© Springer-Verlag GmbH Germany, part of Springer Nature 2018

## Abstract

The *Ponte delle Torri* is a large medieval masonry bridge, one of the main architectural heritage of Spoleto, Italy. The location of the bridge is less than 50 km from the main epicenters of the recent Central Italy earthquakes ( $M_w > 5.0$ ) that occurred between August 2016 and February 2017. In addition, some minor quakes of the sequence ( $M_w$  between 3.0 and 4.0) occurred within 10 km from the bridge, causing some damages and fear among the population around Spoleto. In this context, the present paper aims at contributing to understand the effects on the structural health of the bridge by analyzing the ambient vibration data acquired before, during and after the seismic sequence, as changes in the dynamic behavior of the structure might indicate the evolution of the state of damage of the monument. In particular, vibration data were processed by modal analysis techniques for mutual validation of the extracted modal parameters. Environmental and vibration data were simultaneously acquired to take into account the seasonal effects on the dynamic behavior. Through a preliminary finite-element model (FEM) the modal shapes were obtained to choose the positions where to locate the sensors for the vibration spot acquisition session of June 2015. The same positions were acquired in October 2016 and at the end of May 2017. Subsequently, a more detailed FEM was produced based on a 3D reconstruction by structure-from-motion stereo-photogrammetry technique with high-resolution photos from unmanned aerial vehicle of the bridge. The model was validated through comparison with the damage pattern experienced by the bridge and then used for assessing the seismic safety by means of both, nonlinear dynamic and static push-over analyses.

**Keywords** Structural health monitoring · Historic structures · Ambient vibration testing · Central Italy earthquakes · Earthquake engineering · FEM

---

✉ Ivan Roselli  
ivan.roselli@enea.it

Marialaura Malena  
marialaura.malena@uniroma3.it

Marialuisa Mongelli  
marialuisa.mongelli@enea.it

Nicola Cavalagli  
nicola.cavalagli@unipg.it

Massimiliano Gioffrè  
massimiliano.gioffre@unipg.it

Gerardo De Canio  
gerardo.decanio@enea.it

Gianmarco de Felice  
gianmarco.defelice@uniroma3.it

<sup>1</sup> ENEA, Italian National Agency for New Technologies, Energy and Sustainable Economic Development, Casaccia R. C, Via Anguillarese 301, 00123 S. Maria Di Galeria, Rome, Italy

<sup>2</sup> Department of Engineering, Roma Tre University, Via Vito Volterra 62, 00146 Rome, Italy

<sup>3</sup> Department of Civil and Environmental Engineering, University of Perugia, via G. Duranti 93, 06125 Perugia, Italy

## 1 Introduction

According to the scientific community and as recently stated also in the Italian National Guidelines for the assessment and the reduction of the seismic risk of the cultural heritage [1] the structural health monitoring (SHM) plays a crucial role to integrate and support conservation strategies for the historic architectural assets. SHM aims to give, at every moment during the life of a structure, a diagnosis of the “state” of the constituent materials, of the different parts, and of the full assembly of these parts constituting the structure as a whole [2]. In particular, continuous or periodic surveys, preferably conducted by non-destructive testing (NDT) techniques, given the relevance of the artistic and historical value of ancient buildings, can provide valuable contribution.

In this context, the ambient vibration testing is to be considered a NDT able to supply information on the global health of the structure through the investigation of its dynamic behavior. More specifically, this kind of testing methodology aims at identifying the modal parameters, which might change over time either for changes in environmental conditions (especially in terms of temperature) or for a degradation of the structural health. Consequently, the effects of the environmental conditions must be taken into account to assess the modal parameters of the construction. Through the contemporary measurement of ambient vibration and temperature several examples in literature demonstrated the practical feasibility of such damage detection methods for flexible structures, like towers, vaults, domes and large bridges [3–6].

The above SHM methodology can be used to check the state of damage of structures after a hazardous event, like a seismic event or, sometimes, a series of seismic events, such as in the case of a long lasting sequence with several major shakes, as occurred in the recent 2016–2017 Central Italy sequence.

In the present paper the ambient vibration monitoring of the Ponte delle Torri was carried out in three spot measurement sessions with a so-called roving-sensors approach [7], acquired in June 2015, in October 2016 and at the end of May 2017.

The above data were processed through several modal analysis techniques to assess the reliability of the results by mutual validation of the extracted modal parameters. A preliminary finite-element model (FEM) was created for obtaining indications on the positions where to locate the sensors for the vibration acquisitions. Subsequently, a more detailed FEM was produced on the basis of a geometry survey with high-resolution stereo-photogrammetric photos of the bridge taken from a drone. The detailed FEM was calibrated using the modal frequencies extracted from data

acquired in the first experimental session of June 2015 to have updated numerical model before the seismic sequence. Nonlinear dynamic analyses of the bridge under the main shakes of the Central Italy sequence from August 2016 to October 2017 were carried out. The model is then validated by comparison with the damage survey of the bridge after the seismic events. Eventually, further nonlinear push-over analyses were carried out using the N2 method [8], aiming at assessing the seismic safety of the bridge according to actual standards.

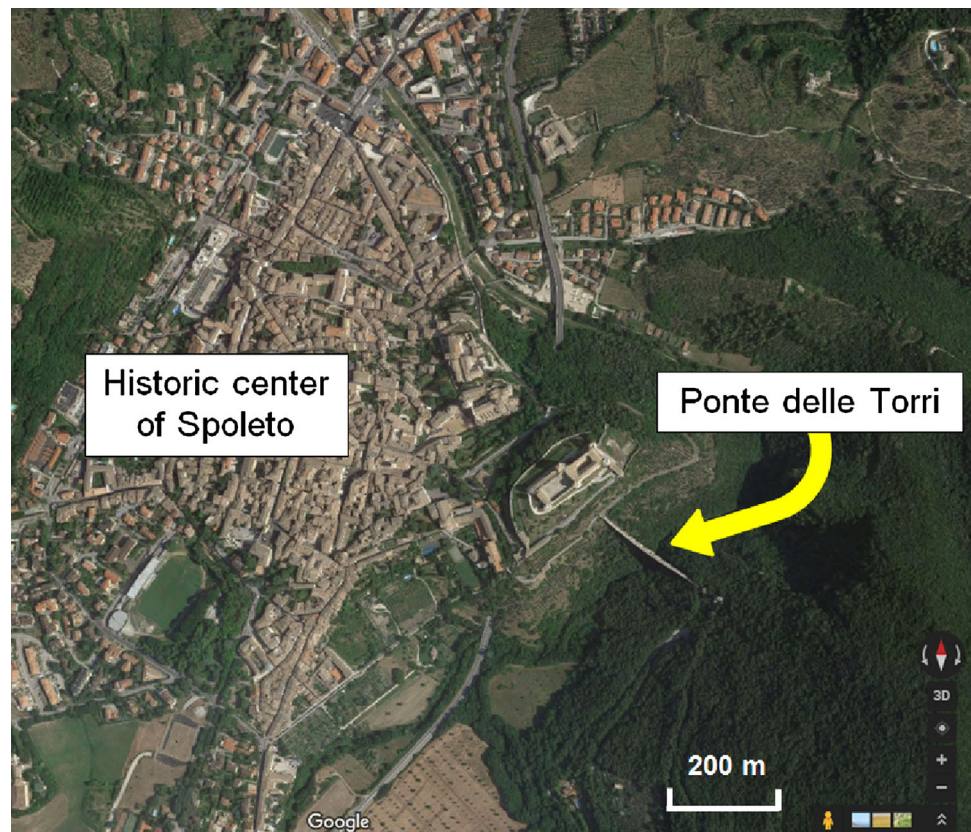
### 1.1 Historical notes

The Ponte delle Torri (Fig. 1) connects Sant’Elia hill (the hill that hold the Rocca Albornoziana fortress) and mount Monteluco, located East from the historic center of Spoleto (Fig. 2). It was mainly built in the 13th or 14th century, presumably exploiting some existing ruins of previous structures, inherited from the Etruscan or the Roman period, for the foundations [9]. Such previous structures were likely fortified towers (“Torri” in Italian) and constitute part of some present-day piers that support the deck by ogive arches. On the deck a road-way was built, which is used today as a pedestrian walkway for promenades. In the following centuries, the bridge was also used as an aqueduct: a water canal was obtained on top of a wall built instead of the parapet on the south side of the bridge with a proper height and slope that allowed water flowing by gravity. This wall was initially continuous until 1845 when, under gonfalonier Parenzi, a wide semicircular window was opened at halfway of the deck. In 1891 the Ponte delle Torri was still a key element of the water network system that served Spoleto. Three pipelines supplied water to the bridge that conveyed it to two water mills and then to the city.



Fig. 1 View from northeast of the Ponte delle Torri of Spoleto

**Fig. 2** Satellite view of the Ponte delle Torri and of the historic center of Spoleto



## 1.2 The bridge structure

The studied structure is a large ten-arcade historic masonry bridge. The construction has a structure with abutments and piers (“towers”) made up of rubble walls in a square matrix assembled by mortar and lime. It has an overall length of about 230 m, while the highest tower is over 70 m [10]. The structure is only apparently regular in materials and shapes. In fact, piers and arches have all different shapes and sizes. In particular, the piers closer to Monteluco are thicker and the arches are raised about half of their height, while the piers closer to Sant’Elia hill present the longest clear span of the bridge. In addition, the parts of the bridge towards Sant’Elia and Monteluco present differences in the masonry texture, as a consequence of their different construction timings or succeeding rebuilding and restoration interventions. In particular, in the one closer to Sant’Elia hill, the masonry appears well-arranged, with precise squared stones at the corners, generally well interconnected, typical of a successive period with respect to the rougher and poorer masonry characterizing the other side of the bridge towards Monteluco, especially in the bottom of the piers.

The most recent wall is the one supporting the water canal on the south side. Its thickness is about 2.00 m and its height over the deck is variable, as it follows the inclination

needed for water flowing. Its masonry is very heterogeneous in materials and typology.

The bridge showed a widespread and extended state of damage already prior to the Central Italy sequence. The presence of several cracks had already been detected in previous inspections and investigations [11, 12]. Such cracks seemed mostly to be related to the heterogeneity of the construction materials, as usually befalls to ancient structures that are subjected to a series of structural interventions, architectural modifications, and functional changes during their long history. The upper part of the piers is generally made up of better quality masonry with mortar of good consistency. In the lower piers, widespread damages caused the expulsion of some cornerstones, local dislocations of the masonry, and some partial detachments of the outer layers. The fourth pier from West displayed two very large cracks that are clearly visible [12].

The state of preservation of the piers towards Sant’Elia hill is better and the clamping edge is also good. The top of the arches, especially those on the slope of Monteluco, shows evidence of heavy water infiltrations that ingenerated losses of mortar binder and some skiving of the wall apparatus, along with the formation of cracks and peeling of the outer frames at the intrados of the arches. Moreover, some arches exhibit typical effects of biotic aggression, with particular severity in the less exposed areas.

Occasionally, also some serious deterioration of walls materials was evidenced.

## 2 Modal identification

### 2.1 Preliminary FEM and sensors setup

A preliminary finite-element model (FEM) was created with NASTRAN hexa-8 elements. The mechanical properties of the masonry were assumed hypothesizing, in first approximation, a homogeneous isotropic elastic material with mechanical properties deduced from recent tests and investigations [11]. The adopted values for the material properties were: Young's modulus  $E = 8000 \text{ N/mm}^2$ , Poisson's ratio  $\nu = 0.3$ , and density  $\rho = 2067 \text{ kg/m}^3$ . The boundary conditions at the base of the piers were taken perfectly clamped for simplicity.

The above preliminary FEM was used to obtain the modal frequencies and shapes of the first modes. The modal shapes were obtained to determine the positions where to locate the sensors for the ambient vibration acquisitions carried out from June 2015 to May 2017. The first four modes resulted being bending modes in the transversal direction ( $y$  direction in Fig. 3) with also a torsional component in the fourth mode. The sensors for the ambient vibration acquisitions were mainly located on the bridge deck for accessibility reasons, but also a few measurement points were acquired at the central piers bases. The sensors were positioned exploiting the potentialities of the roving-sensors approach, or multi-setup measurements strategy (MSMS) [7]. Such strategy is able to provide reliable estimates of modal parameters through operational modal analysis (OMA) techniques [13], especially if multi-setup data are merged in a pre-identification step. In particular, recent studies [7] found that modal frequencies can be estimated with the same accuracy level

with respect to simultaneous measurements, while the estimation of modal damping ratios is slightly rougher. MSMS permits to limit the number  $m$  of utilized instruments according to the following equation:

$$m = \frac{(p - r)}{n} + r \quad (1)$$

where  $n$  is the number of setups,  $p$  is the total number of measurement points of which  $r$  remain unchanged in all setups. In the present work, we could acquire 17 positions with only three instruments in eight test setups, by roving two instruments while keeping the position of the third one unchanged as reference for all setups (Fig. 4).

The used instrumentation comprised three SARA Instruments SL06 recorders equipped with triaxial electrodynamic velocimeters. Each setup was acquired at a 200 Hz sampling frequency for a recording time  $t$  of 20 min ( $t = 1200 \text{ s}$ ), so that as suggested by recent studies [14], the minimum natural frequency detectable by OMA techniques without deteriorating modal identification accuracy is given by  $200/t$  corresponding to 0.17 Hz, which is much lower than first mode frequency of 0.6 Hz predicted in first approximation by the preliminary FEM. As the reference sensor was staying in the same positions during all setups, it basically measured the mode shapes in this position over and over, while other sensors were moved to different positions on the bridge. Such reference position was determined as the measurement point, where the modes of interest (the first four modes) were supposed to have the highest response level, according to preliminary FEM estimates, which resulted to be the top of the central pier of the bridge. This multi-setup configuration was acquired on 3rd June 2015 [15]. The recorded data were analyzed through OMA techniques, which proved to be very effective and consolidated in identifying the natural response of bridges [16, 17].

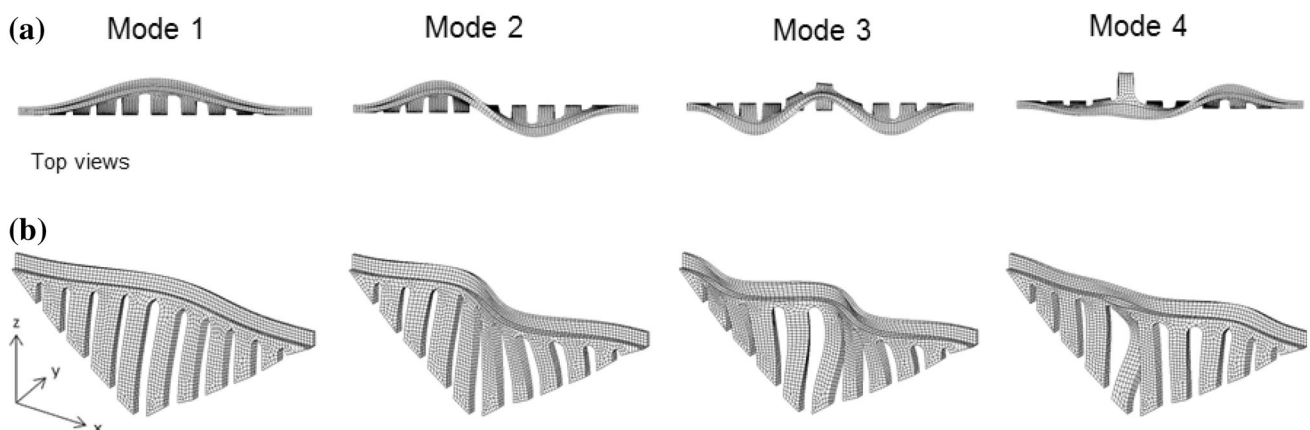
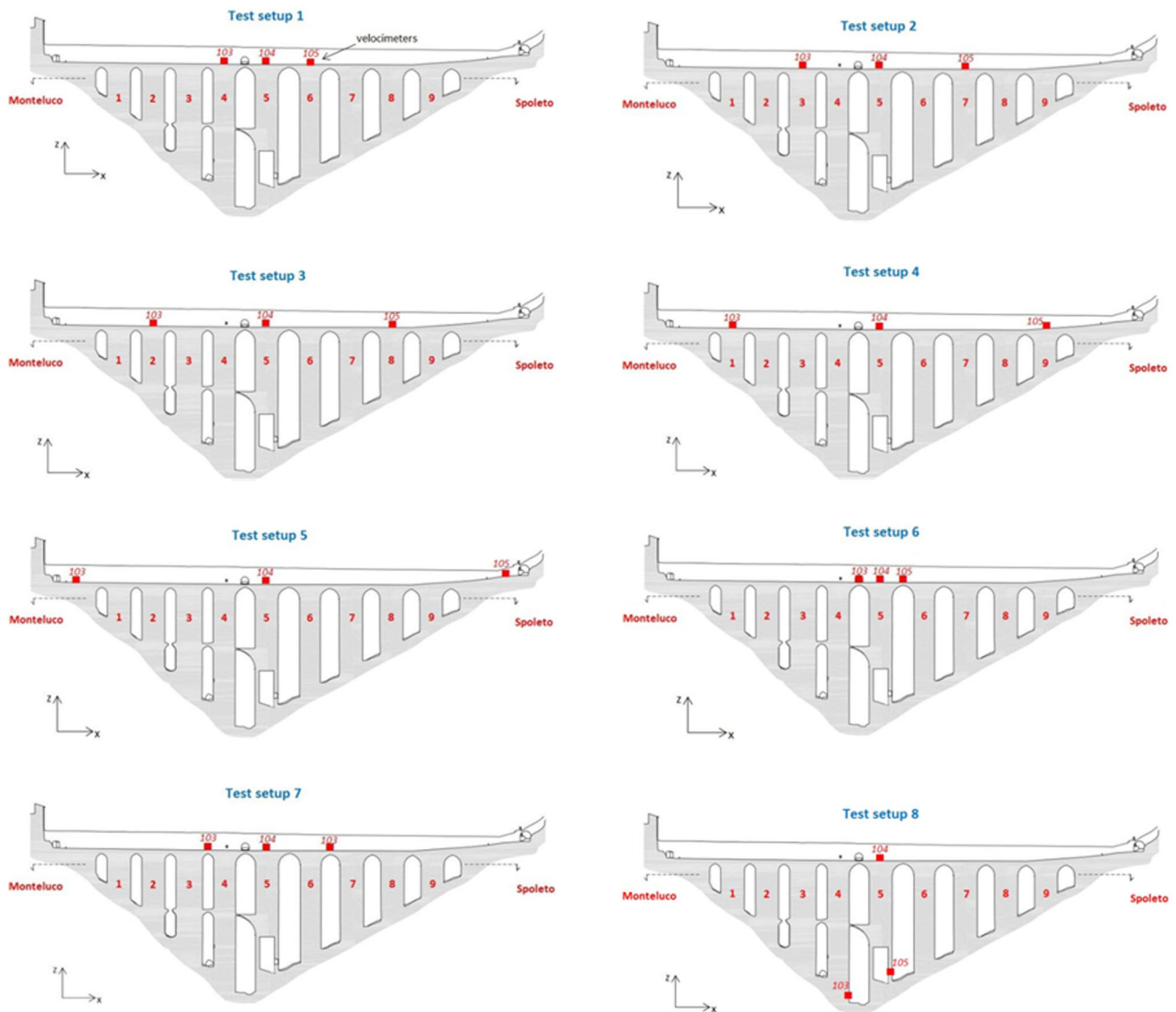


Fig. 3 Modal shapes from preliminary FEM with NASTRAN hexa-8 elements: top views (a), perspective view (b)



**Fig. 4** Positions of velocimeters (103, 104 and 105) in ambient vibration acquisition setups 1–8 of 3rd June 2015

## 2.2 Modal analysis techniques

The ambient vibration data were processed by several modal analysis techniques to have a mutual validation of the results. The MSMS data were handled through the ARTeMIS Modal Pro software [18], which is capable of pre-identification merging of setups. Among the several OMA techniques, the frequency-domain decomposition (FDD) [19], the enhanced frequency-domain decomposition (EFDD) [20], and the stochastic subspace identification (SSI) [21] were utilized. FDD is a basic technique, extremely easy to use, that utilizes the singular value decomposition (SVD) of the estimated spectral densities of the measured response. Modes are identified by manually picking the peaks in SVD plots calculated from the spectral density spectra of the responses. As the FDD technique is

based on using a single frequency line from the FFT analysis, the accuracy of the estimated natural frequency depends on the FFT resolution and no modal damping is calculated. The EFDD technique is an extension to the FDD in which the SDOF Power Spectral Density function, identified around a peak of resonance, is taken back to the time domain using the Inverse Discrete Fourier Transform (IDFT). The natural frequency is obtained by determining the number of zero-crossing as a function of time, and the damping by the logarithmic decrement of the corresponding SDOF normalized auto correlation function.

Different from the previous ones, SSI is a time-domain technique and is based on an unconditionally linear least squares estimation of the model obtained by ambient vibration data. In particular, in the present study, a Crystal Clear SSI algorithm was used, which helps to get clear

results leading to cleaner and more stable stabilization diagrams.

In Fig. 5, the mode estimation by OMA-SSI of data acquired on 3rd June 2015 and related accuracy is shown.

In addition, experimental modal analysis (EMA) approach based on the frequency response function (FRF) was considered. In particular, data acquired at abutments were taken as input signals and the others as output signals. The FRF was calculated in terms of transmissibility function defined as the ratio of the cross spectral density of input and output signals by the auto spectral density of the input [22]. In particular, the output signal was recorded in central position on the deck in transversal direction, while the abutment located on the Sant’Elia hill was taken as input. Then, a 6-Degree-of-Freedom (6DOF) synthetic FRF curve was obtained by means of the modal model parameters values associated with the first five identified modes. The model considers three parameters: the FRF peak values, the resonant frequencies, and the non-dimensional modal damping. The above synthetic FRF is a complex function, fitting the experimental FRF on the basis of the number of desired DOFs and on the modal participation masses estimates associated at each identified mode. The graph of Fig. 6 shows the synthetic FRF obtained from data of 3rd June 2015.

Another analysis capable of providing indications on modal frequencies is the horizontal-to-vertical spectral ratio (HVSR) at each triaxial velocimeter [23]. HVSR is calculated as the ratio between the amplitude of the Fourier spectra of horizontal and vertical components of triaxial data recorded on the deck of the bridge. It is an empirical technique able to provide rough estimates of natural frequencies on the basis of the hypothesis that vertical vibration travels through the structure without significant amplification in comparison with the horizontal

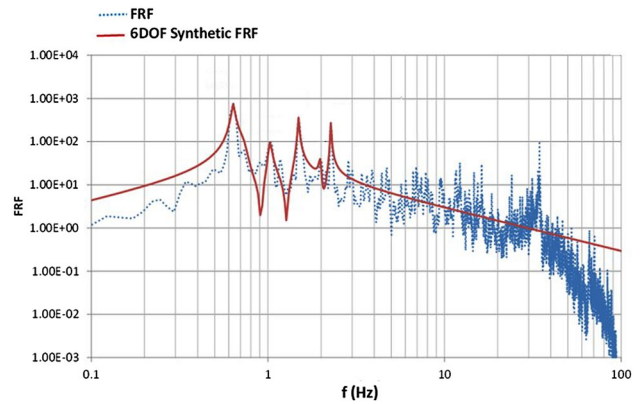


Fig. 6 Identification of modal frequencies by FRF of data acquired on 3rd June 2015 in the central position of bridge deck with reference to the abutment on the Sant’Elia hill

components, which are much more amplified. In practice, this assumption remains substantially valid for bending modes in transversal directions when soil–structure interaction are negligible, as in the case of ambient vibrations.

Applying several techniques made possible to evaluate the reliability of the results by mutual validation. In particular, the statistical dispersion of the results derived from different methods can be considered to evaluate the convergence towards mutual validated and, thus, more reliable results. To such purpose, the variance of data was calculated as an indicator of statistical dispersion. Given the operational conditions during data collection, EMA and HVSR techniques are expected to be provide estimates of the modal parameters with a higher level of approximation than OMA techniques. For this reason, results from EMA and HVSR techniques were used only for a qualitative comparison of the modal frequencies, while average and variance of values from OMA techniques for quantitative

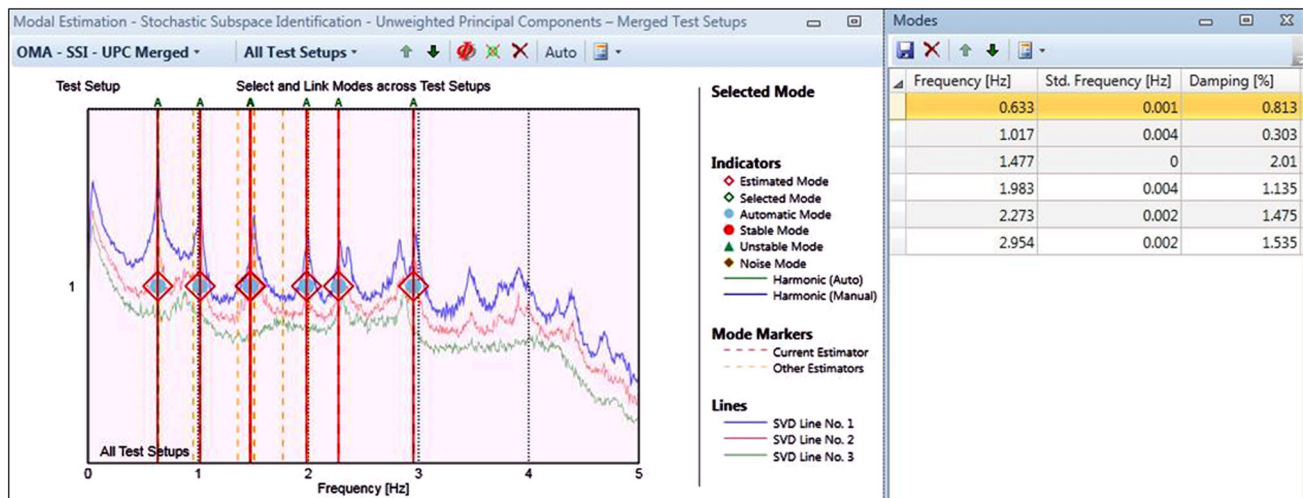


Fig. 5 Identification of modal frequencies by OMA-SSI of data acquired on 3rd June 2015: mode estimation diagrams (left) and accuracy (right)

evaluation of modal parameters. The first four modal frequencies and damping values obtained by all modal analyses of the vibration data acquired during the experimental session of 3rd June 2015 are illustrated in Table 1. Since the damping acts as mode coupling nonlinear energy transfer operator, its overestimation below the half-power level is due to the graphic reconstruction of the curve when a reduced number of modes are considered. Nevertheless, the obtained synthetic FRF reconstruction is sufficient to assess the structural response of the tower bridge by mean of the 6DOF modal model extracted parameters. The frequencies of the second and third modes by OMA-EFDD technique of 3rd June 2015 were ignored, because their complexity values were quite high ( $> 10\%$ ), and consequently, their reliability was low. Mode complexity values are computed as the convex hull area of the components of the  $i$ th eigenvector in the complex plane in relation with a unitary circle (complexity plot) [24]. The average values and related variances of modal frequencies and modal damping values calculated by OMA techniques are also reported in Table 2 to evaluate the reliability of the applied techniques. As the values of variance were always lower than 0.001 Hz, the average values of the calculated frequencies by OMA can be considered very consistent.

The values of modal damping in Table 1 show a certain dispersion. In fact, damping in historic masonry, as well as in other structures, is known to have high uncertainty and is remarkably dependent on the intensity of the dynamic excitation [25], which is essentially due to wind conditions during ambient vibration acquisitions. Moreover, damping values extracted through FRF were calculated by half-

power bandwidth method, which is known to overestimate damping in multi-degree-of-freedom structures. Even considering only the values from EFDD and SSI techniques, values of variance are relatively high (Table 2), so they should be taken as only rough indications. Consequently, as a general indication, the damping of the first four modes can be realistically estimated to be lower than 1%. In the numerical analyses, the adopted value of damping was 0.6% (average value neglecting the third mode that shows a much higher variance).

Along with the ambient vibration data, also environmental data were acquired to take into account of the seasonal effects on the dynamic behavior of the studied bridge. As well known, environmental changes, especially in terms of temperature, can influence the mechanical properties of the materials. Consequently, their effects need to be effectively investigated and taken into account when assessing the changes of modal parameters values over time for a reliable structural health monitoring [26].

### 2.3 Geometry and crack pattern survey

A geometry reconstruction of the bridge was obtained by processing high-resolution stereo-photogrammetric photos taken from UAV. A very light multicopter SenseFly Exom drone equipped with ultrasonic and circular vision sensors performed a complete photogrammetric scanning of the bridge in December 2015. The photos were georeferenced thanks to a GPS module embedded in the drone. A total amount of 818 photos at 38 Mpixels (respectively, 411 of the north side and 407 of the south side of the bridge) were taken with a ground sample distance (GSD) equal to 1.75 mm/pixel. Considering an average RMS error of about 0.7 pixels, the resulting accuracy was 1.3 mm. The acquired images were post-processed by structure-from-motion (SfM) technique [27], which allows to estimate and reconstruct 3D structures from two-dimensional images. It performs photogrammetric processing of digital images and generates 3D spatial data and a dense-point cloud useful for visual effects production and indirect measurements of the objects.

Some pictures were excluded for their low quality, so that, finally, 393 images were considered for the north side and 343 images for the south side (Fig. 7). However, because of the still big quantity of data, the images were divided into two different groups, which were processed separately with PhotoScan software [27]. After that, the two resulting dense-point clouds were aligned and merged in a unique dense cloud [28].

The 3D reconstruction was post-processed through the ENEA HPC resources provided by CRESCO infrastructure (Research Computational Center on Complex Systems) [29].

**Table 1** First four modal frequencies and damping % obtained with all applied modal analysis techniques in the experimental session of 3rd June 2015, before the Central Italy seismic sequence

Modal frequencies (Hz)					
2015-06-03 session					
Mode	FRF	OMA-FDD	OMA-EFDD	OMA-SSI	HVSR
1	0.634	0.635	0.634	0.633	0.628
2	1.022	1.021	–	1.017	1.035
3	1.513	1.509	–	1.477	1.480
4	2.000	1.997	2.030	1.983	1.950
Modal damping (%)					
2015-06-03 session					
Mode	FRF*	OMA-EFDD	OMA-SSI		
1	1.500	0.629	0.813		
2	0.730	0.424	0.303		
3	0.630	0.464	2.010		
4	1.070	0.547	1.135		

\*Half-power bandwidth method

**Table 2** Average and the variance of the first four modal frequencies and damping % obtained with applied OMA techniques in the experimental session of 3rd June 2015, before the Central Italy seismic sequence

Modal frequencies (Hz)					
2015-06-03 session					
Mode	OMA-FDD	OMA-EFDD	OMA-SSI	Average	Variance
1	0.635	0.634	0.633	0.634	0.000001
2	1.021	–	1.017	1.019	0.000008
3	1.509	–	1.477	1.493	0.000512
4	1.997	2.030	1.983	2.003	0.000582
Modal damping (%)					
2015-06-03 session					
Mode	OMA-EFDD	OMA-SSI	Average	Variance	
1	0.629	0.813	0.721	0.016928	
2	0.424	0.303	0.364	0.007321	
3	0.464	2.010	1.237	1.195058	
4	0.547	1.135	0.841	0.172872	

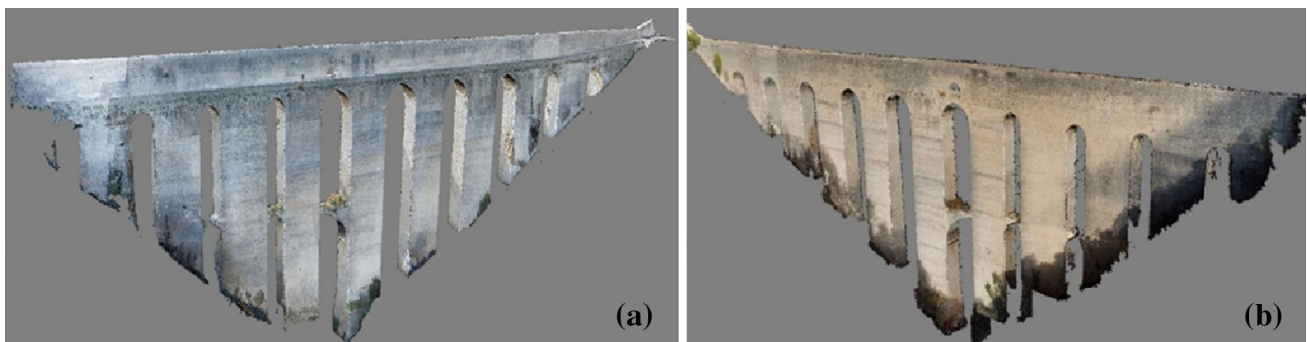


**Fig. 7** Dense clouds by SfM of north (a) and south (b) sides of the bridge

Thanks to georeferencing, the reconstructed model turned out geometrically correct. A check was carried out to verify the accuracy of the 3D reconstruction by matching the measures physically obtained during the experimental campaign to the measures of the numerical model.

Two different 3D reconstructions were obtained, by two dense cloud point with different types of definition (number of points), and consequently, two polygonal mesh models were derived: the former one with 150,000 faces for the geometric survey, while the latter has 18 million faces and was used for the identification of the crack pattern. In particular, a map of the state of damage was created with the cracks taxonomical defined and an identification code was assigned. The cracks were described through several properties, such as their length, start/end position, and an indication of the damage class according to the macroseismic European EMS98.

The 3D photogrammetric reconstruction gave additional information about the structure: the dimensions of each pier resulted different in section and high, and the foot of the piers also showed an enlargement (Fig. 8). Based on

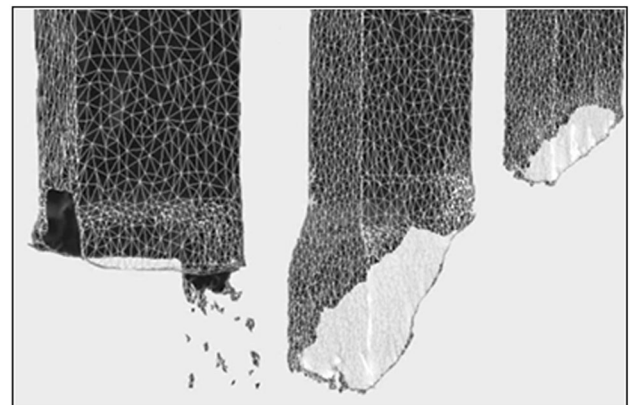
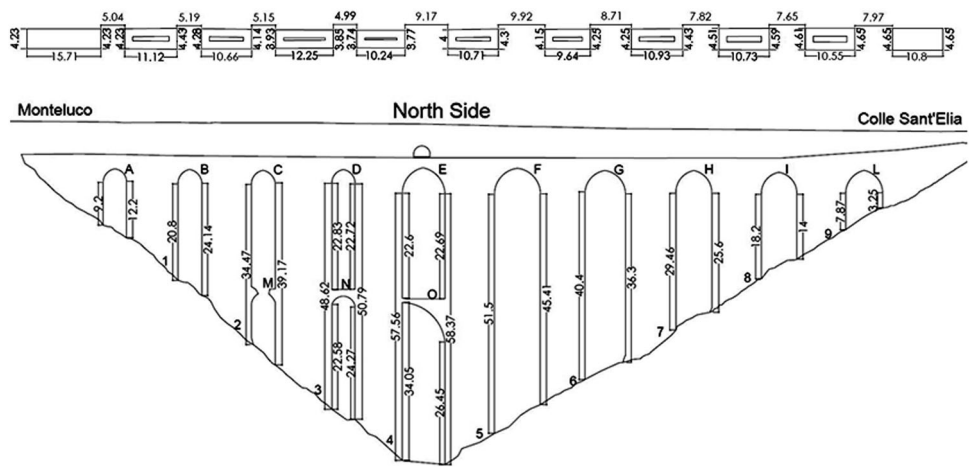


**Fig. 8** Detail of the bases of piers 4, 5 and 6 (from left to right)

the geometric survey obtained by the photogrammetric scanning, it was possible to define a new CAD model (Fig. 9). Arches were labeled with letters (from A to O) and piers with numbers (from 1 to 9).



**Fig. 9** CAD model based on the 3D photogrammetric survey



**2.4 Finite-element model**

The 3D geometric reconstruction of the bridge was used to modify the preliminary FEM into a more detailed FEM.

Furthermore, in agreement with some previous destructive test executed on the bridge, such as simple and double flat jack tests [10], the sections of the pier were modeled as hollow, with a wall thickness of 1.5 m.

A calibration of the detailed FEM was performed by comparison of its numerical modal frequencies with the corresponding results of the dynamic identification carried out in the first experimental session. FEM calibration was optimized, minimizing the difference between FEM modal frequency and corresponding experimental value for the first mode, which is characterized by the highest mass participation (about 44%), while for the higher frequencies (having mass participations of 5% or less), a residual error in the order of 10–12% was accepted (Table 3). Basically, a slight overestimate of higher frequencies can be due to the fact that the crack pattern and, in general, the state of the damage (that was not modeled in the FEM) affected more higher modes than the first one. The final material properties assigned to the calibrated FEM are shown in Table 4. In Fig. 10, the comparison of the first four modes from experimental data and FEM simulation by Modal

**Table 4** Final material properties for calibrated FEM

<i>E</i> (MPa)	<i>v</i>	$\rho$ (kg/m <sup>3</sup> )
8000	0.2	2107

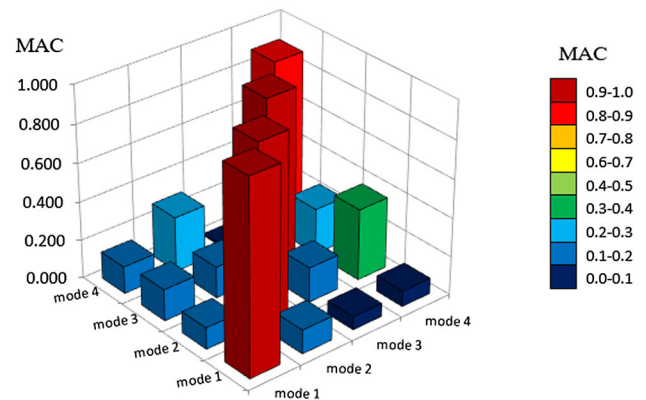


**Fig. 10** Comparison of the first four modes from experimental data and FEM simulation by modal assurance criterion (MAC)

**Table 3** Modal frequencies by calibrated FEM and experimental results by OMA of 3rd June 2015

Mode	Frequency (Hz)		
	FEM	Experimental	$\Delta$ (%)
1	0.629	0.634	– 0.8
2	1.129	1.019	10.8
3	1.672	1.493	11.9
4	2.195	2.003	9.6

Assurance Criterion (MAC) [30] is shown. The modal shapes obtained by OMA techniques were very similar to the ones simulated by FEM (Fig. 11).

The finite-element model of the bridge was developed using 4-node solid elements for an overall total number of nodes and elements equal to 61,889 and 265,064, respectively. The nonlinear mechanical behavior of masonry was modeled by means of the concrete damage plasticity (CDP) material model, which is available within the Abaqus software. Even though in the literature, more appropriate nonlinear masonry models are available [31–34] and the CDP was conceived for isotropic brittle materials like concrete, it was extensively used also for quite anisotropic materials such as masonry through a parameters’ adaptation [35, 36]. The CDP model allows the analysis of materials with different strengths in tension and in compression, assuming different damage parameters. The

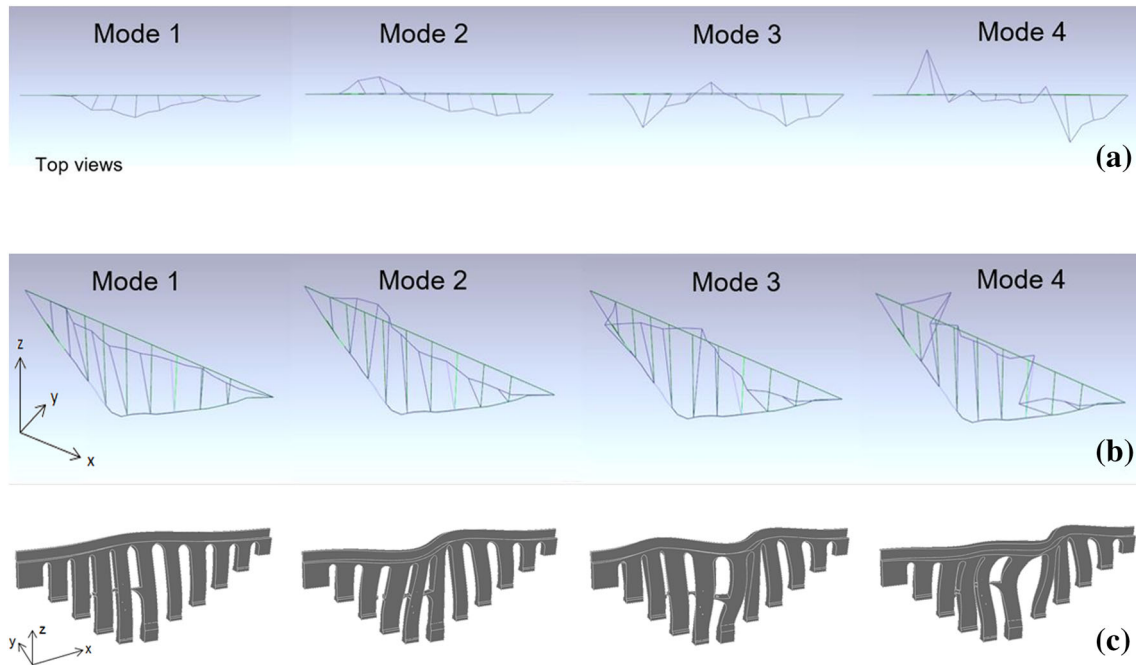


**Fig. 11** First four modal shapes obtained by OMA-FDD analysis: top views (a), perspective view (b). Modal shapes of the first four modes by calibrated FEM (c)

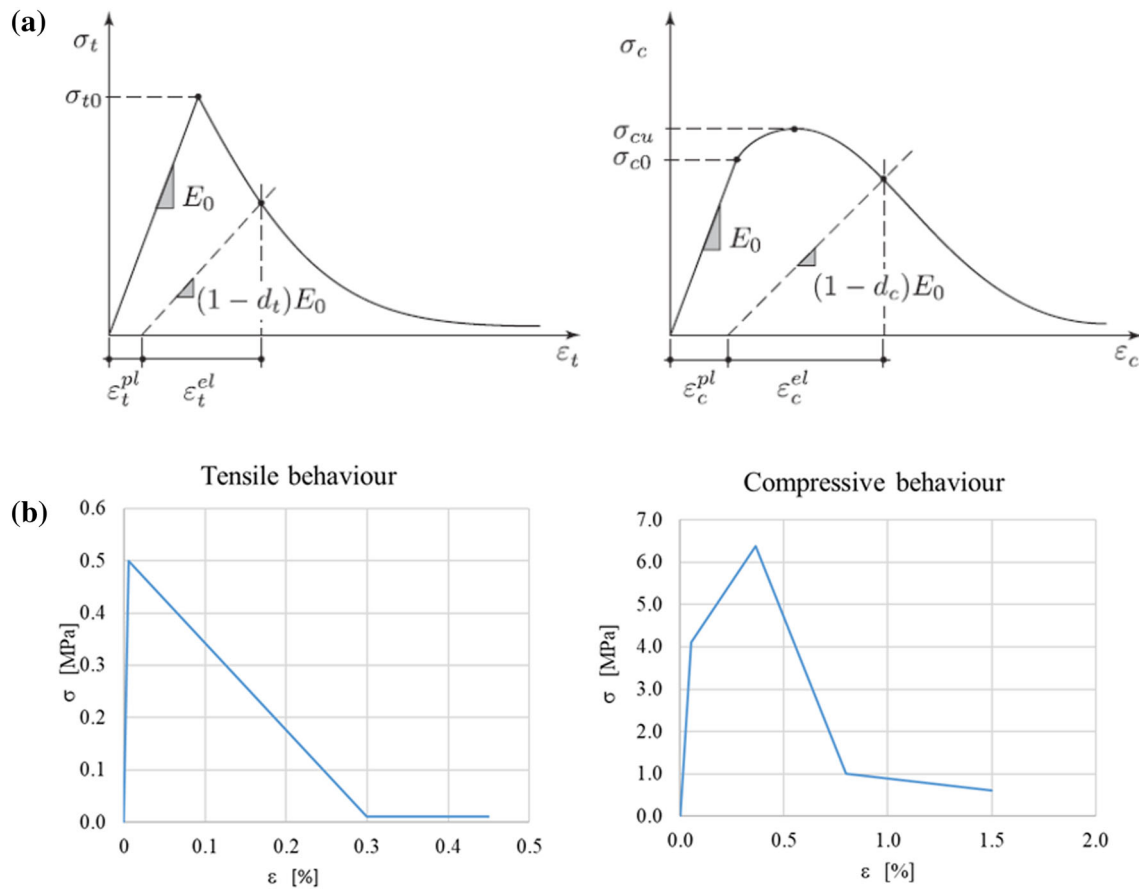


**Fig. 12** Constitutive material laws (a) and masonry mono-axial behavior in tension and in compression (b)

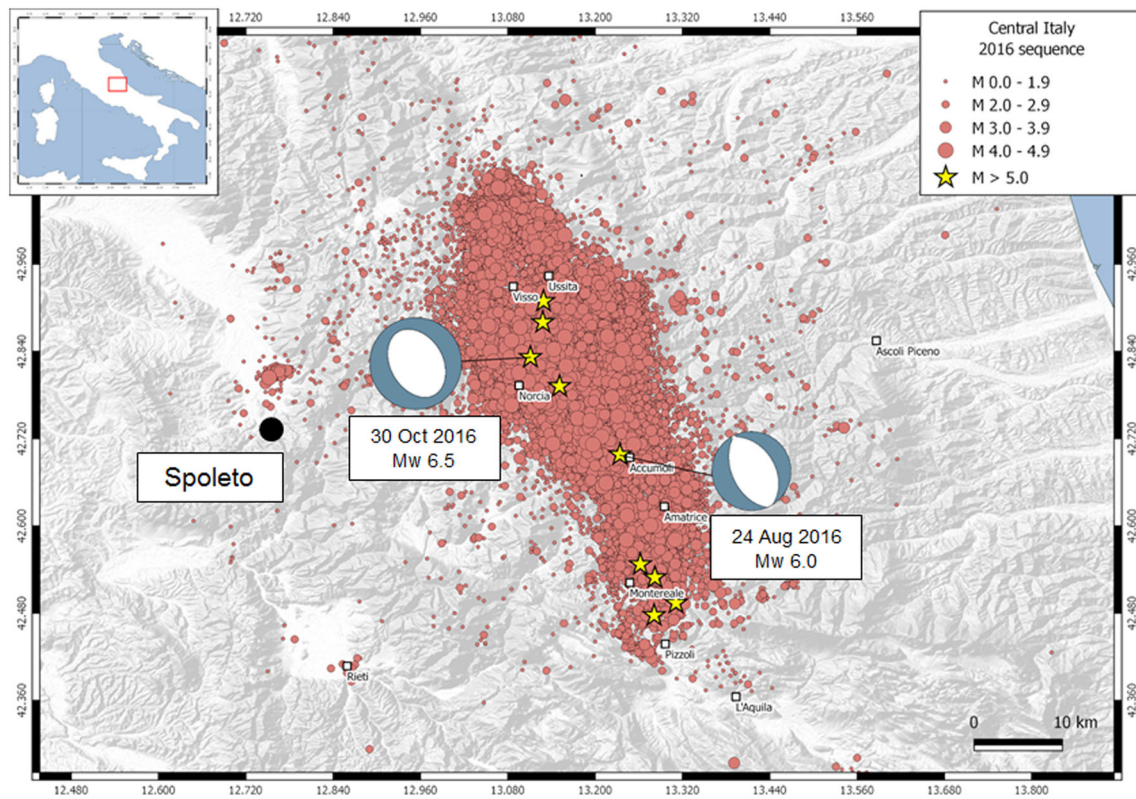


Fig. 13 Location of Spoleto with respect to the epicenters of Central Italy seismic sequence from 24th August 2016 to 20th February 2017. The two largest events of the sequence are enhanced

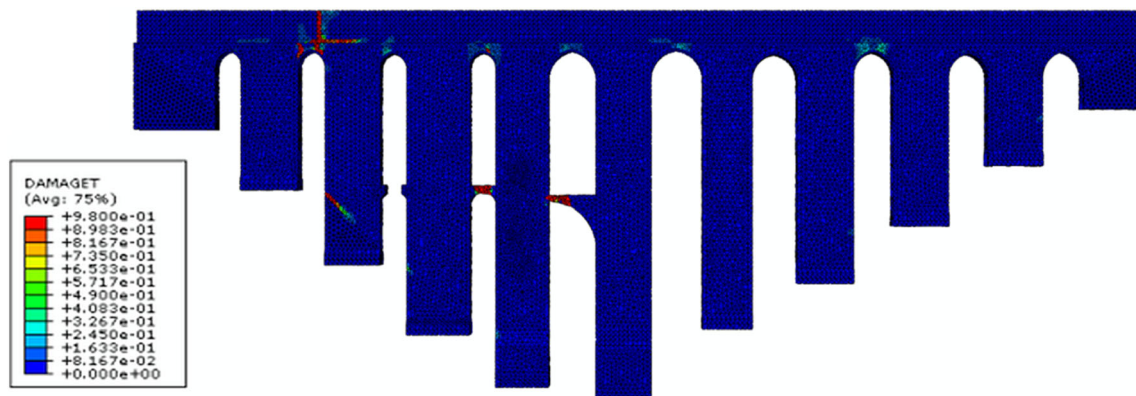


Fig. 14 Tensile damage distribution obtained by mean of the FE model after the application of the Central Italy 2016–2017 seismic sequence

behavior in tension is linear elastic up to the stress peak  $\sigma_{t0}$  is reached. Afterwards, micro-cracks start to propagate in the material and the stress–strain curve drops down following a softening branch. Under axial compression, the response is linear up to the yield stress  $\sigma_{c0}$ , then hardening usually occurs before compression crushing initiates, which is represented by a softening branch beyond the peak stress  $\sigma_{cu}$  (Fig. 12a). The decay rate at which the curves decrease is defined by the damage variable  $d_t$  and  $d_c$ , in tension and in compression, respectively. The nonlinear

constitutive laws in compression and tension adopted in this work are (Fig. 12)

$$\sigma_t = (1 - d_t)E_0(\varepsilon_t - \varepsilon_t^{pl}) \tag{2}$$

$$\sigma_c = (1 - d_c)E_0(\varepsilon_c - \varepsilon_c^{pl}) \tag{3}$$

where  $\sigma_t$  and  $\sigma_c$  are the mono-axial tensile and compressive stress,  $E_0$  is the initial Young Modulus,  $\varepsilon_t$  and  $\varepsilon_c$  are the total strain in tension and in compression, and  $\varepsilon_t^{pl}$  and  $\varepsilon_c^{pl}$  are the equivalent plastic strain in tension and in compression.

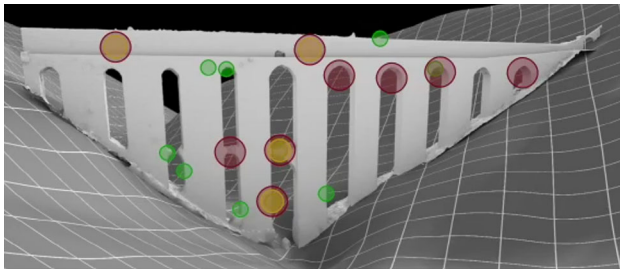


**Fig. 15** Damage survey of the bridge after the Central Italy 2016–2017 seismic events provided by the Spoleto Municipality (red circles). Preexisting damage (green and yellow circles) were repaired in previous restoration interventions

The strength domain is defined by a standard Drucker–Prager surface modified with a  $K_c$  parameter representing the ratio between the distance from the hydrostatic axis of the maximum compression and tension, respectively [35]. The value of  $K_c$  has been kept equal to  $2/3$ . Furthermore, a regularization of the tensile corner was assumed in the constitutive law by mean of the eccentricity parameter. Such a parameter indicates the rate at which the plastic flow potential approaches the asymptote, i.e. the flow potential tends to a straight line as the eccentricity tends to zero. The default value equal to 0.1 was adopted. For what

concerns the dilatation angle, a value of  $10^\circ$  was adopted for the inelastic deformation in the nonlinear range, in agreement with experimental evidences available in the literature. The ratio between the bi-axial,  $f_{b0}$ , and mono-axial,  $f_{c0}$ , compression strength has been kept equal to 1.16 as suggested in [37]. Furthermore, the CDP model overcomes convergences difficulties, and typical of numerical analyses carried out adopting material models exhibiting softening behavior and stiffness degradation, using a viscoplastic regularization of the constitutive equations. A viscosity parameter equal to 0.002 was adopted, which is sufficiently small if compared to the characteristic time increment, in the way to not compromise the results, in agreement with [35] and [36]. Finally, the damping ratio adopted in the analyses was obtained from the analysis of the ambient vibrations data.

## 2.5 The 2016–2017 Central Italy seismic sequence

Between August 2016 and February 2017, a series of moderate-to-large earthquakes occurred along a 60-km-long Apenninic-trending normal-fault system [38]. This fault system was activated during the night of 24 August

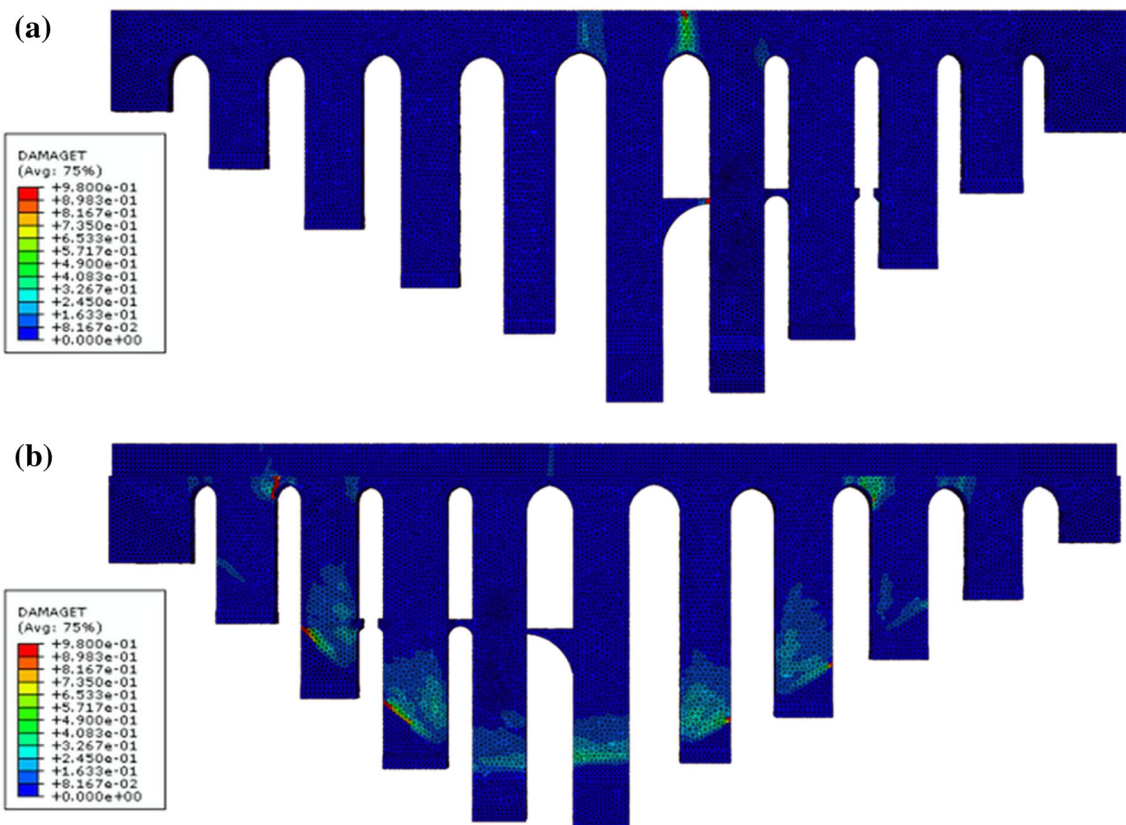


**Fig. 16** Tensile damage in the bridge derived from push-over analysis with horizontal forces consistent with the first modal shape of the structure: south side of the bridge (a); north side of the bridge (b)

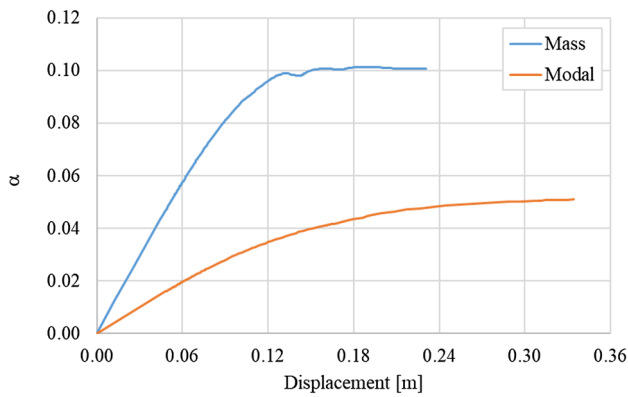


**Fig. 17** Push-over analysis: the ratio  $\alpha$  between the base shear and self-weight is plotted vs the out-of-plane displacement of the middle span of the bridge deck

when a Mw-6.0 event with epicenter located near the town of Amatrice quaked central Italy causing 299 casualties and severe damages to structures and infrastructures in the area. Subsequently, other six shakes with Mw > 5.0 were recorded, worsening and extending the damages to structures and infrastructures with further collapses in the already hit area and in the surroundings of the new epicenters.

The severity of such consequences was so catastrophic because of the high seismic vulnerability of the local constructions (mainly poor and historic masonry) and of the shallowness of the largest events, having an estimated depth of 8–10 km. In particular, the largest event (Mw 6.5) occurred on 30 October at a depth of 9.2 km, but fortunately caused no casualties, because the population had already abandoned the most vulnerable and damaged areas that had been hit just 4 days before by another Mw 5.9 earthquake. Then, the energy of the sequence diminished, but still from March to July 2017, many quakes between Mw 3.0 and Mw 4.0 occurred.

As for the studied bridge, it is located 20-km East–South–East from the epicenter of the 30 October event and

within 50 km from all 64 epicenters with Mw > 4.0 of the sequence. Moreover, also eight minor quakes of the sequence with Mw between 3.0 and 4.0 occurred within 10 km from the bridge, a couple of which caused some limited damages and fear among the population around Spoleto. The location of Spoleto with respect to the epicenters of the Central Italy sequence is shown in Fig. 13.

## 3 Numerical analyses

### 3.1 Nonlinear dynamic

Several nonlinear FE numerical analyses of the given bridge were carried out by mean of the FEM code Abaqus with the inelastic constitutive model previously defined. For the nonlinear dynamic analysis under time-history acceleration, the main shocks of the Central Italy sequence on 24 August 2016 and 30 October 2016 were adopted as seismic input. In particular, the accelerograms recorded by the seismic station of Monteluco, which is very close to the bridge, were considered. In Fig. 14, the distribution of the tensile damage in the bridge derived from the sequence of the seismic events is reported. Aiming at validating the developed model, the results in terms of tensile damage were compared with the damage survey conducted after the seismic sequence. In Fig. 15, the damages registered after the recent seismic sequence are represented, highlighted by red circles, while green and yellow circles are related to the previous events, following which the bridge was subjected to restoration. Numerical analyses localized the most severe tensile damages in correspondence of the two little arches N and O connecting the central piers of the bridge. Less severe damages were also simulated at the upper part of the big arches, especially arches D, F, and H towards Sant’Elia hill. The analyses provided also relevant tensile damage of the wall on the top of bridge in correspondence of arch B, where damages previously occurred (yellow

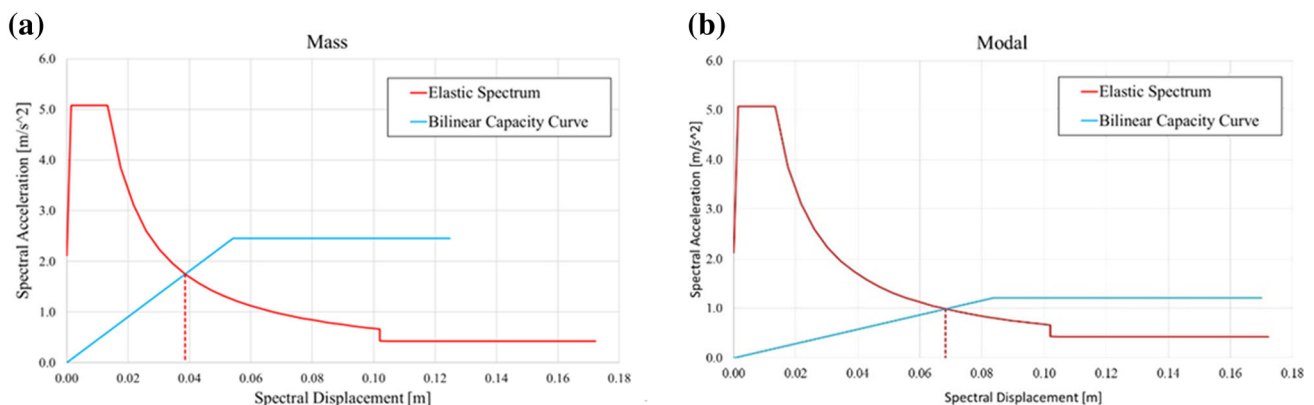


**Fig. 18** N2 safety assessment: mass (a) and modal (b)

**Table 5** First four modal frequencies and damping % obtained with all applied modal analysis techniques in the experimental sessions 13th October 2016 and 29th May 2017

Modal frequencies (Hz)					
2016-10-13 session					
Mode	FRF	OMA-FDD	OMA-EFDD	OMA-SSI	HVSR
1	0.618	0.610	0.612	0.612	0.611
2	0.971	0.972	0.970	0.971	0.982
3	1.429	1.421	1.421	1.421	1.407
4	1.868	1.860	1.872	–	1.834
2017-05-29 session					
Mode	FRF	OMA-FDD	OMA-EFDD	OMA-SSI	HVSR
1	0.629	0.632	0.631	0.632	0.630
2	1.023	1.006	1.014	1.014	1.066
3	1.498	1.497	1.496	1.494	1.483
4	1.990	1.976	1.976	1.973	1.939
Modal damping (%)					
2016-10-13 session					
Mode	FRF*	OMA-EFDD	OMA-SSI		
1	1.050	0.634	0.404		
2	0.669	0.908	0.664		
3	1.365	0.475	0.747		
4	0.910	0.580	–		
2017-05-29 session					
Mode	FRF*	OMA-EFDD	OMA-SSI		
1	2.703	0.434	0.401		
2	2.004	0.549	0.534		
3	1.502	0.377	0.545		
4	0.650	0.395	1.500		

\*Half-power bandwidth method

circle), but then were repaired. Hence, the above analyses are in good accordance with the observe damage.

### 3.2 Push-over analyses

Once the FE model was validated, push-over analyses were carried out, aiming at evaluating the seismic vulnerability of the bridge. According to the Italian Guideline, two push-over analyses were performed, the first one under horizontal forces proportional to the mass and the second one under horizontal forces consistent with the first modal shape. This latter acts in the transversal direction according in agreement with the modal identification and has a

participating mass of 44%. The push-over analyses were carried out applying the self-weight of the bridge, in a first step, and keeping it constant, in a second step, when the horizontal forces in the transversal direction were applied. In Fig. 16, the results of the push-over analysis with horizontal forces proportional to first modal shape are represented in terms of maximum plastic strains distribution over the structure. It is worth noting that no plastic strains in compression developed, and that both push-over analyses gave rise to similar damage distributions. In Fig. 17, the push-over curves are plotted as the ratio between the base shear and the weight of the bridge versus the transversal displacement of the control point located at the middle span of the bridge deck. As expected, the load pattern of the first mode provides the lower capacity of the structure, due to the greater arm of the stress resultant with respect to the base of the piers.

Finally, the displacement-based procedure using non-linear static push-over analysis, according to the N2 method, was used to assess the seismic safety of the bridge. The adopted elastic spectrum is the one provide by the Italian Guideline for the site of the bridge. As shown in Fig. 18, the check made by the N2 safety assessment method is fully fulfilled.

### 3.3 Analysis of the ambient vibration tests during the seismic sequence

The same positions of the bridge as in 2015 were recorded on 13th October 2016 and on 29th May 2017. The same configurations were acquired and the same modal analysis techniques were applied to these vibration data. The results in terms of modal frequencies and damping values are illustrated in Table 5, while the corresponding average and variance values by OMA for each mode can be observed in Table 6, which confirm the mutual validation that was found for data of 2015. Figure 19a shows the identification of modal frequencies by OMA-EFDD of data acquired on 29th May 2017.

The frequencies of the first four modes are depicted in Fig. 19b for all three acquisition sessions. They decreased slightly from 2015 to October 2016, but in May 2017, they returned very close to the values obtained in June 2015. In Fig. 20, the recorded temperatures during the three ambient vibration acquisitions are illustrated: the minimum (at about 10 a.m. local time), maximum (at about 2 p.m.), and average temperature values are put into evidence. Average values were used in the following calculations, making a maximum error of about 2 °C. As shown in Fig. 21, during June 2015 and May 2017 sessions, air temperature

**Table 6** Average and the variance of the first four modal frequencies and damping % obtained with applied OMA techniques in the experimental sessions of 13th October 2016 and 29th May 2017

Modal frequencies (Hz)					
2016-10-13 session					
Mode	OMA-FDD	OMA-EFDD	OMA-SSI	Average	Variance
1	0.610	0.612	0.612	0.611	0.000001
2	0.972	0.970	0.971	0.971	0.000001
3	1.421	1.421	1.421	1.421	0.000000
4	1.860	1.872	–	1.866	0.000072
2017-05-29 session					
Mode	OMA-FDD	OMA-EFDD	OMA-SSI	Average	Variance
1	0.632	0.631	0.632	0.632	0.000000
2	1.006	1.014	1.014	1.011	0.000021
3	1.497	1.496	1.494	1.496	0.000002
4	1.976	1.976	1.973	1.975	0.000003
Modal damping (%)					
2016-10-13 session					
Mode	OMA-EFDD	OMA-SSI	Average	Variance	
1	0.634	0.404	0.519	0.026450	
2	0.908	0.664	0.786	0.029768	
3	0.475	0.747	0.611	0.036992	
4	0.580	–	0.580	–	
2017-05-29 session					
Mode	OMA-EFDD	OMA-SSI	Average	Variance	
1	0.434	0.401	0.418	0.000544	
2	0.549	0.534	0.542	0.000113	
3	0.377	0.545	0.461	0.014112	
4	0.395	1.500	0.948	0.610513	

conditions were very similar, as well as the values of the identified modal frequencies, displaying well-fitted correlations for all considered modes. The latter suggests that in the explored temperature range (10–30 °C), a simple auto-regression (AR) procedure [39] or a support vector machine (SVM) method [40] might be appropriate for damage detection, though more data should be collected for more solid statistical analysis or more refined methods, such as the ones by principal component analysis (PCA) [41], or better, by multi-variate linear or dynamic regression [5, 42]. The above results indicate that air temperature could be the main responsible of the slight changes detected in the modal frequencies during the seismic sequence, even if some visible damages were observed by visual inspection after the seismic events of the sequence, as reported in Fig. 15 (red circles). Such damages had evidently limited impact on the overall behavior of the structure. In particular, the main damage was represented

by some stones collapsed from the arches N and O, which give very limited contribution to the stiffness of the overall structure, and could significantly affect only very local response, represented by higher modes than the first four ones. In addition, the cracks surveyed at the intrados of the arches F, G, H, and L towards Sant’Elia hill probably play a limited role. They might involve only the most external layers of the masonry without affecting significantly the structural behavior of the arches.

## 4 Conclusions

Among the several available techniques able to provide information on the structural health of historic masonry constructions, the dynamic identification through modal analysis of ambient vibration acquisitions is one of the most effective tools to obtain indications on the global

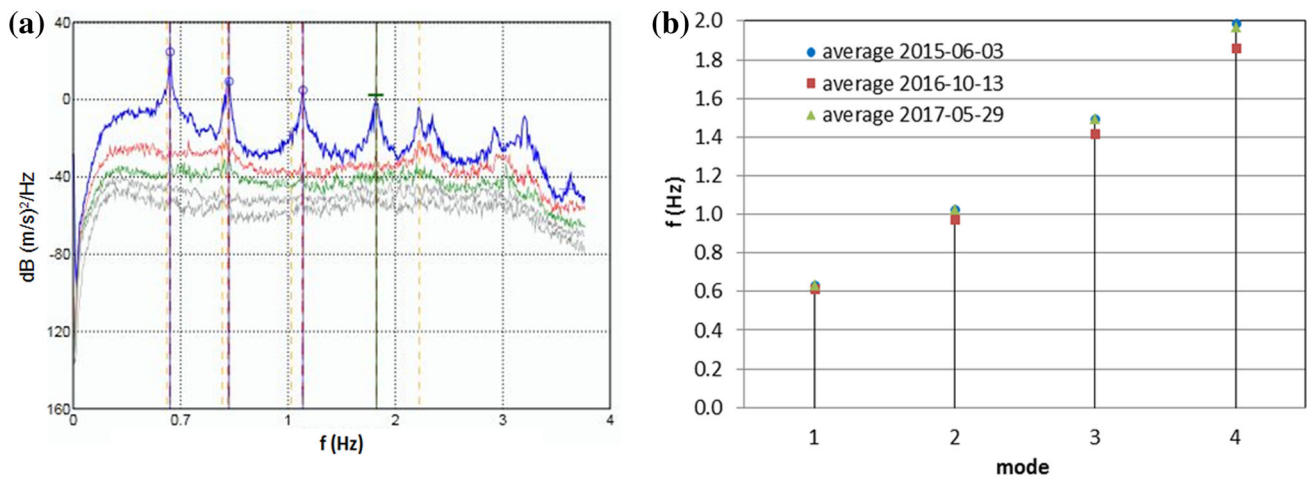


**Fig. 19** Identification of modal frequencies by OMA-EFDD of data acquired on 29th May 2017 (a). Average values of the first four modal frequencies obtained by ambient vibration acquisitions of 2015–2017 experimental sessions (b)

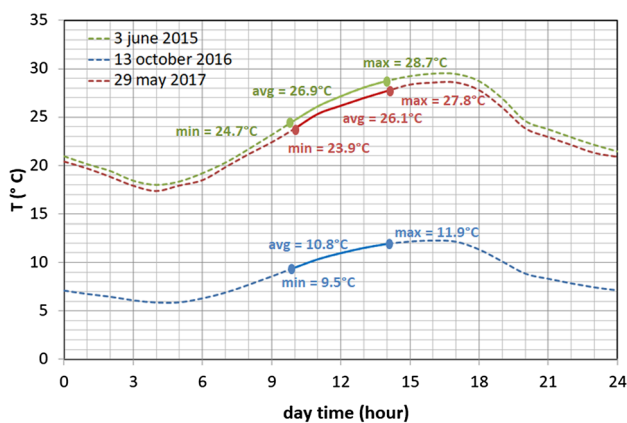


**Fig. 20** Air temperature  $T$  recorded during vibration test acquisitions (start and final time of acquisitions, at around 10 a.m. and 2 p.m., respectively, are indicated). Minimum (min), average (avg) and maximum (max) temperature values are indicated for each acquisition date

response. Combining such dynamic identification procedures with contemporary data of environmental parameters (particularly, the temperature), a deeper knowledge of the structural behavior of the studied structure could be achieved and a very effective monitoring of the overall structural health could be reached. On the other hand, in the case of cultural heritage assets, the aesthetic value of the structure is so much valuable that also limited or local damages that do not affect significantly the structural behavior of the monument (plasters, cladding, veneers, non-structural members, etc.) should be taken into account and should be investigated with other techniques. In the case of the studied bridge, some damages were surveyed by visual inspections conducted after the Central Italy seismic

sequence, but their actual relevance on the overall stability of the structure needed to be investigated.

In the present paper, three ambient vibration tests, acquired with a so-called roving-sensors approach from June 2015 to May 2017, of the Ponte delle Torri were processed and analyzed. The modal parameters were extracted with several EMA and OMA techniques to evaluate the mutual validation of the results through their variance. The variance was very low in terms of frequencies ( $< 0.001$  Hz), while damping results were more dispersed, but still in acceptable agreement, given the high uncertainties and inaccuracies characterizing this parameter.

The modal frequencies noticeable decreased in October 2016 (decays of 3–7%), which was the first acquisition session carried out after the beginning of Central Italy earthquake sequence (24 August 2016 shake of Mw 6.0). However, in May 2017 session, the modal frequencies substantially returned to their initial values of June 2015, which were obtained in very similar seasonal and, consequently, environmental conditions, as confirmed by air temperature data. This suggests that the October 2016 decrease was essentially due to the effect of the different environmental conditions, though more experimental data would be necessary for more solid statistical analysis. In particular, the frequencies seemed to increase with the temperature in the observed range (10–30 °C), which is a reasonable result and a quite common finding in this kind of structures.

Furthermore, the conducted numerical analyses gave encouraging indications on the safety assessment of the bridge. Importantly, such indications were based on the use of a detailed FEM calibrated with the modal frequencies



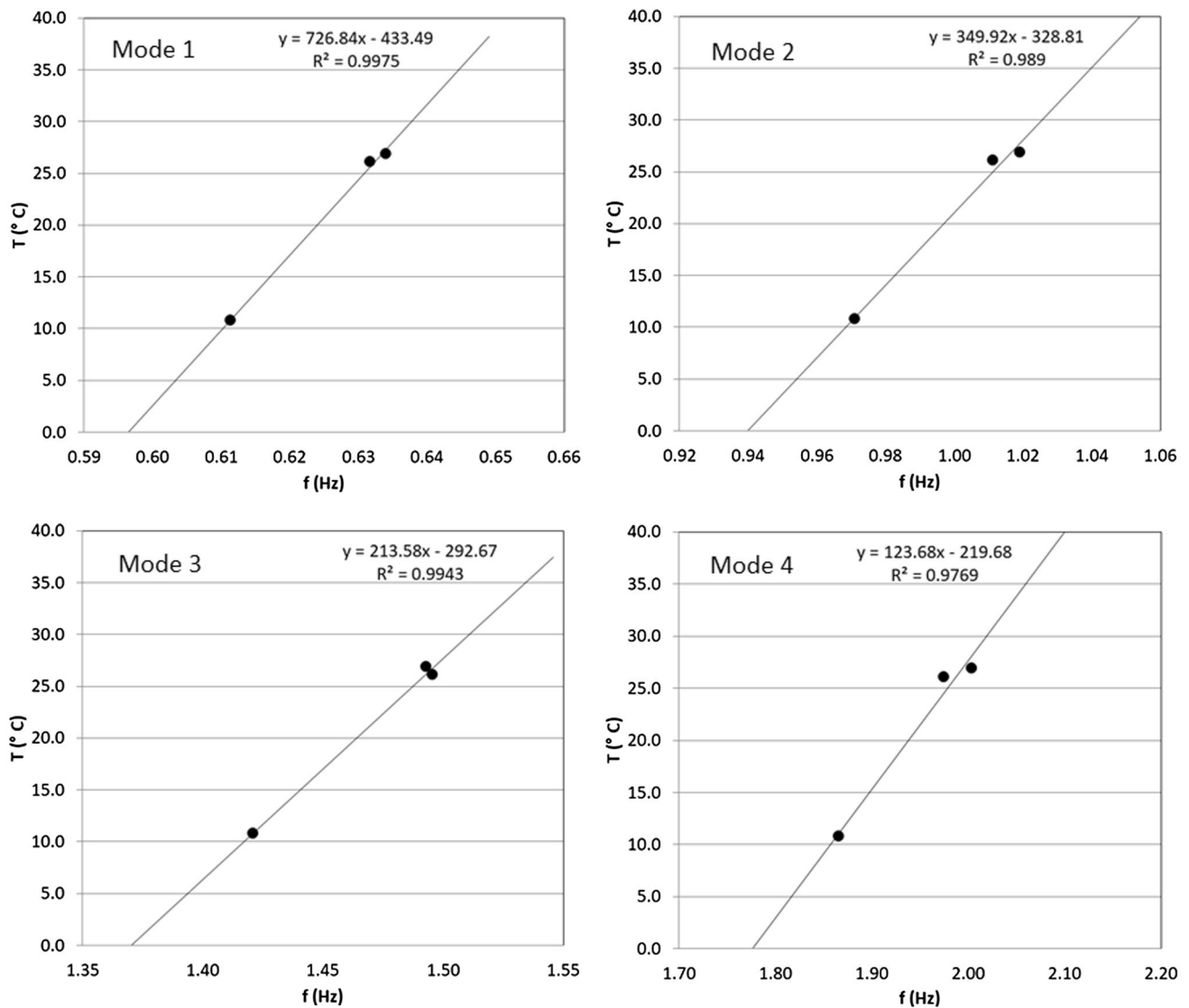


Fig. 21 Correlation of first four modal frequencies obtained in 2015–2017 acquisitions with the local air temperature  $T$

from on-site experimental data and validated by comparison of the numerical tensile damage with the damage surveyed on the field, which resulted in a very good agreement.

## References

- Italian Presidency of the Council of Ministers (2008) Direttiva del presidente del Consiglio dei Ministri per la valutazione e la riduzione del rischio sismico del patrimonio culturale con riferimento alle norme tecniche per le costruzioni, Suppl. Ord. alla Gazzetta ufficiale, n. 24, 29 gennaio 2008 [in Italian]. Rome, Italy: Istituto Poligrafico della Zecca di Stato
- Balageas D, Fritzen CP, Güemes A (2006) Structural health monitoring. ISTE Ltd., London
- De Stefano A, Matta E, Clemente P (2016) Structural health monitoring of historical heritage in Italy: some relevant experiences. *J Civil Struct Health Monit* 6(1):83–106
- Saisi A, Gentile C, Guidobaldi M (2015) Post-earthquake continuous dynamic monitoring of the Gabbia Tower in Mantua, Italy. *Constr Build Mater* 81:101–112
- Gentile C, Guidobaldi M, Saisi A (2016) One-year dynamic monitoring of a historic tower: damage detection under changing environment. *Meccanica* 51(11):2873–2889
- Cavalagli N, Comanducci G, Ubertini F (2017) Earthquake-induced damage detection in a monumental masonry bell-tower using long-term dynamic monitoring data. *J Earthq Eng.* <https://doi.org/10.1080/13632469.2017.1323048>
- Orlowitz E, Andersen P, Brandt A (2015) Comparison of simultaneous and multi-setup measurement strategies in operational modal analysis. In: 6th International operational modal analysis conference (IOMAC'15), Gijon, Spain, 12–14 May 2015
- Fajfar P (2000) A nonlinear analysis method for performance-based seismic design. *Earthq Spectra* 16(3):573–592

9. Gentili L, Giacché L, Ragni B, Toscano B (1978) L'Umbria. Manuali per il Territorio. Spoleto, Roma, pp 432–434
10. Sansi A (1984) Storia del comune di Spoleto, vol I–VIII. Accademia Spoletina, Spoleto
11. Gioffrè M, Gusella V, Cluni F (2008) Performance evaluation of monumental bridges: testing and monitoring 'Ponte delle Torri' in Spoleto. *Struct Infrastruct E* 4(2):95–106
12. Coccetta M, Marchetti M, Marziani M, Scatolini G (2013) Il ponte delle Torri progetto preliminare e lotto fun-zionale per il consolidamento ed il restauro. Comune di Spoleto
13. Raineri C, Fabbrocino G, Cosenza E (2007) Automatic operational modal analysis as structural health monitoring tool: theoretical and applications aspects. *Key Eng Mater* 347:479–484
14. Ruzzo C, Failla G, Collu M, Nava V, Fiamma V, Arena F (2016) Operational modal analysis of a spar-type floating platform using frequency domain decomposition method. *Energies* 9(11):870
15. De Canio G, Mongelli M, Roselli I, Tati A, Addressi D, Nocera M, Liberatore D (2016) Numerical and operational modal analyses of the "Ponte delle Torri", Spoleto, Italy. In: 10th international conference on structural analysis of historical constructions, Leuven, Belgium, 13–15 September 2016
16. Brincker R, De Stefano A, Piombo B (1996) Ambient data to analyse the dynamic behaviour of bridges: a first comparison between different techniques. In: 14th international modal analysis conference (IMAC), Dearborn, USA, 12–15 February 1996
17. Araiza Garaygordobil JC (2004) Dynamic identification and model updating of historical buildings. State-of-the-art review. In: 4th international seminar on structural analysis of historical constructions, Padua, Italy, 10–13 November 2004
18. SVS (2013) ARTeMIS Modal Pro software 2013. <http://www.svibs>
19. Brincker R, Zhang L, Andersen P (2001) Modal identification of output-only systems using frequency domain decomposition. *Smart Mater Struct* 10:441–445
20. Jacobsen NJ, Andersen P, Brincker R (2006) Using enhanced frequency domain decomposition as a robust technique to harmonic excitation in operational modal analysis. In: Proceedings of ISMA2006: international conference on noise & vibration engineering, Leuven, Belgium
21. Peeters B, De Roeck G (2001) Stochastic system identification for operational modal analysis: a review. *J Dyn Syst Meas Control* 123:659–667
22. Maia N, Silva J (1998) Theoretical and experimental modal analysis. Research Studies Press, Baldock
23. Gallipoli MR, Mucciarelli M, Vona M (2009) Empirical estimate of fundamental frequencies and damping for Italian buildings. *Earthq Eng Struct D* 38(8):973–988
24. Ewins DJ (2000) Modal testing: theory, practice and application. Research Studies Press, Philadelphia
25. Elmenhawi A, Sorour M, Mufti A, Jaeger LG, Shrive N (2010) Damping mechanisms and damping ratios in vibrating unreinforced stone masonry. *Eng Struct* 32(10):3269–3278
26. Ubertini F, Comanducci G, Cavalagli N, Pisello L, Materazzi L, Cotana F (2017) Environmental effects on natural frequencies of the San Pietro bell tower in Perugia, Italy, and their removal for structural performance assessment. *Mech Syst Signal Process* 82(1):307–322
27. Verhoeven G (2011) Taking computer vision aloft—archaeological three-dimensional reconstructions from aerial photographs with Photoscan, *Archaeol. Prospection* 18:67–73
28. Mongelli M, De Canio G, Roselli I, Malena M, Nacuzi A, de Felice G (2017) 3D Photogrammetric reconstruction by drone scanning for FE analysis and crack pattern mapping of the "Bridge of the Towers", Spoleto. In: mechanics of masonry structures strengthened with composite materials (MuRiCo5), Bologna, Italy, 28–30 June 2017
29. Ponti G, Palombi F, Abate D, Ambrosino F, Aprea G, Bastianelli T, Beone F, Bertini R, Bracco G, Caporicci M, Calosso B, Chinnici M, Colavincenzo A, Cucurullo A, D'Angelo P, De Rosa M, De Michele P, Funel A, Furini G, Giammattei D, Giusepponi S, Guadagni R, Guarnieri G, Italiano A, Magagnino S, Mariano A, Mencuccini G, Mercuri C, Migliori S, Ornelli P, Pecoraro S, Perozziello A, Pierattini S, Podda S, Poggi F, Quintiliani A, Rocchi A, Sciò C, Simoni F, Vita A (2014) The role of medium size facilities in the HPC ecosystem: the case of the new CRESCO4 cluster integrated in the ENEAGRID infrastructure. In: International conference on high performance computing and simulation (HPCS), Bologna, Italy, 21–25 July 2014
30. Pastor M, Binda M, Harčarik T (2012) Modal assurance criterion. *Procedia Eng* 48:543–548
31. Lourenco PB, Rots JG (1997) Multisurface interface model for analysis of masonry structures. *J Eng Mech* 123(7):660–668
32. Berto L, Saetta A, Scotta R, Vitaliani R (2002) An orthotropic damage model for masonry structures. *Int J Numer Methods Eng* 55(2):127–157
33. de Felice G, Amorosi A, Malena M (2010) Elasto-plastic analysis of block structures through a homogenization method. *Int J Numer Anal Methods Geomech* 34(3):221–247
34. Pelà L, Cervera M, Roca P (2011) Continuum damage model for orthotropic materials: application to masonry. *Comput Methods Appl Mech Eng* 200(9):917–930
35. Valente M, Milani G (2016) Seismic assessment of historical masonry towers by means of simplified approaches and standard FEM. *Constr Build Mater* 108:74–104
36. Castellazzi G, D'Altri AM, de Miranda S, Ubertini F (2017) An innovative numerical modeling strategy for the structural analysis of historical monumental buildings. *Eng Struct* 132:229–248
37. Page AW (1981) The biaxial compressive strength of brick masonry. In: Proceeding of the institution of civil engineers, part 2, vol 71, pp 93–906
38. Chiaraluce L, Di Stefano R, Tinti E, Scognamiglio L, Michele M, Casarotti E, Cattaneo M, De Gori P, Chiarabba C, Monachesi G, Lombardi A, Valoroso L, Latorre D, Marzorati S (2017) The 2016 Central Italy Seismic sequence: a first look at the mainshocks, aftershocks, and source models. *Seismol Res Lett* 88(3):757–771
39. Peeters B, Maeck J, De Roeck G (2001) Vibration-based damage detection in civil engineering: excitation sources and temperature effects. *Smart Mater Struct* 10(3):518–527
40. Ni YQ, Hua XG, Fan KQ, Ko JM (2005) Correlating modal properties with temperature using long-term monitoring data and support vector machine technique. *Eng Struct* 27(12):1762–1773
41. Lenaerts V, Kerschen G, Golinval JC (2003) Identification of a continuous structures with a geometrical non-linearity, part II: proper orthogonal decomposition. *J Sound Vib* 262:907–919
42. Hair J, Anderson R, Tatham R, Black W (1998) Multivariate data analysis. Prentice Hall, New Jersey